Piconewton-millisencond force steps reveal the transition kinetics and mechanism of the double stranded DNA elongation

PicoNewton-Millisecond Force Steps Reveal the Transition Kinetics and Mechanism of the Double-Stranded DNA Elongation

Pasquale Bianco,[†] Lorenzo Bongini,[‡] Luca Melli,[†] Mario Dolfi,[†] and Vincenzo Lombardi[†*]
[†]Laboratorio di Fisiologia, Dipartimento di Biologia Evoluzionistica, Università degli Studi di Firenze, Sesto Fiorentino, Italy; and [‡]Departamento de Fisica Fundamental, Universitat de Barcelona, Barcelona, Spain

ABSTRACT We study the kinetics of the overstretching transition in λ-phage double-stranded (ds) DNA from the basic conformation (B state) to the 1.7-times longer and partially unwound conformation (S state), using the dual-laser optical tweezers under force-clamp conditions at 25°C. The unprecedented resolution of our piezo servo-system, which can impose millisecond force steps of 0.5–2 pN, reveals the exponential character of the elongation kinetics and allows us to test the two-state nature of the B-S transition mechanism. By analyzing the load-dependence of the rate constant of the elongation, we find that the elementary elongation step is 5.85 nm, indicating a cooperativity of ~25 basepairs. This mechanism increases the free energy for the elementary reaction to ~94 k_BT, accounting for the stability of the basic conformation of DNA, and explains why ds-DNA can remain in equilibrium as it overstretches.

INTRODUCTION

Precise characterization of the mechanical properties of double-stranded DNA (ds-DNA) is fundamental for understanding the mechanism of the molecular machines used by cells to duplicate and repair their genome and modulate the accessibility of the genetic information (1,2). In living cells, or in physiological solution in the absence of stress, the basic conformation of ds-DNA is the B-form—that is, with the two strands hydrogen-bonded to form a right-handed double helix, with a periodicity of ~3.5 nm or, with a basepair (bp) separation of 0.33 nm, 10.5 bp. Single biomolecule manipulation allows ds-DNA mechanics to be investigated in the range of forces from a fraction of a picoNewton to over 100 pN, that is in the force range exerted by proteins during their interactions with DNA. At forces smaller than ~10 pN the DNA backbone bends under the influence of random thermal fluctuations (3–8); at forces above ~10 pN, the molecule exhibits the stress-strain relation of an elastic material, until the force attains ~65 pN, when, within a few picoNewtons of force change, it modifies its molecular structure to a new overstretched form (S-form), which is characterized by a length 70% larger than that of the B-form (9,10).

Control of the twist of the ds-DNA molecule (11,12) has shown that its length is extremely sensitive to the degree of twisting, revealing the role of the torque in the structural transition, and that the extended S-form of ds-DNA is characterized by an increase in bp per turn from 10.5 to 33–37 (13,14). Thus, untwisting of ds-DNA accompanies the overstretching transition and the torque defines the force at which the transition occurs, according to a global phase diagram of the various conformations of ds-DNA (13,14). Within the force and torque ranges imposed by length or load perturbations on a molecule that has a nick (a break in the covalent bonds of either of the two sugar-phosphate backbones) or is free to rotate, the phase diagram at equilibrium is limited to the definition of the boundary between the two forms B and S (see Fig. 4 *a* in Sarkar et al. (13)). The relatively small thickness of the line representing the boundary between the B state and the S state indicates that the range of torque and force values necessary to complete the transition (~0.5 k_BT for the torque and ~4 pN for the force) is narrow, consistent with a cooperative mechanism.

In contrast with the above analysis and with evidence that, depending on DNA sequence, ionic strength, and temperature, the transition to the extended form of DNA may or may not imply melting (15), the double-stranded structure of the extended form of DNA has been challenged by the work of other researchers, who concluded that the overstretching transition is due to force-induced melting and separation of the two strands (16,17). Evidence in support of this view is given by the dependence of the force for the overstretching transition on the solution conditions such as temperature, pH, and ionic strength, as well as the presence of hysteresis in the rewinding to the B-form. Melting with strand separation during the overstretching transition has been recently recorded with fluorescence microscopy (18,19). However, the interchange between a basepaired B state and a single-stranded extended state cannot explain the overstretching transition when, as in the range of temperatures below 35°C, 1), hysteresis is asymmetric (the first part of the force-extension curve in the transition region upon release coincides with the force extension curve upon stretch) (9,10,20); and 2), the elastic modulus of the overstretched form is higher than that of both the B-form and single-stranded DNA at the same force (21,22).

Moreover, it has been shown that even ds-DNA that is topologically closed but rotationally unconstrained can undergo the overstretching transition without hysteresis

Submitted May 5, 2011, and accepted for publication June 24, 2011.

*Correspondence: vincenzo.lombardi@unifi.it

Editor: Laura Finzi.

0006-3495/11/08/0866/9 $2.00

doi: 10.1016/j.bpj.2011.06.039

upon relaxation (23). An important contribution to the clarification of these issues has been provided by recent experiments of overstretching under force-clamp: it has been shown that, in agreement with previous findings (15), depending on DNA sequence, salt concentration, and temperature, DNA overstretching may involve either a rapid nonhysteretic transition to the elongated double-stranded S form or a slow hysteretic strand separation (24), and that, even in the presence of nicks and free ends, a stable extended S form of DNA can be generated in physiological conditions (25).

Until now, however, the transition kinetics between compact and extended states of ds-DNA has not been measured. Moreover, existing estimates of the degree of cooperativity of the transition vary by an order of magnitude, the structural and energetic aspects of the B-S transition have not yet been characterized, and the very existence of the double-stranded S state is still questioned (16–18,26–29). Here we describe the force-extension relation of the ds-DNA of λ-phage in physiological solution (150 mM NaCl, 10 mM Tris, 1 mM EDTA, pH 8.0 at 25°C), using a double-laser optical tweezers (10) that can impose on the molecule stress changes made by a staircase of force steps each complete within a few milliseconds and of size 0.5–2 pN via beads attached to opposite strands. Under these conditions, a step stretch applied in the region of forces of the overstretching transition generates an elastic distortion on the molecule. This consists of a transient negative internal torque that induces, in the subsequent few hundreds of milliseconds, an isotonic elongation with an exponential time course that implies untwisting toward a new equilibrium, where the length fraction contributed by the S state is increased at the expense of that contributed by the B state.

Several steps are necessary for the elongation response to complete the overstretching transition, and the kinetics of the elongation response are explained by a simple two-state model in which the DNA molecule is assumed to consist of a series of independent units of ~25 bps that can each flip between two states. The mechanism proposed also reproduces the experimental equilibrium force-extension curves, whose lack of hysteresis shows that the extended S form can be produced in a perfectly reversible way.

MATERIALS AND METHODS

Preparation of DNA

A linearized double-strand λ-DNA (48.5 kbp; New England Biolabs, Ipswich, MA) has been used for the experiments. Single molecules of DNA have been tethered between two streptavidin-coated beads (Spherotech, Libertyville, IL) of either 3.28-μm diameter (17 molecules) or 2.18-μm diameter (4 molecules). For labeling ds-DNA at both ends but on opposite strands, bio-11-dCTP, dATP, dGTP, and dUTP were polymerized opposite the λ-DNA's 12-bp sticky ends using Klenow enzyme. The experiments were made at 25°C in solution with the following composition: 150 mM NaCl, 10 mM Tris, 1 mM EDTA, pH 8.0.

Optical tweezers

Dual-beam optical tweezers (10,30) were used to control both extension and force of single DNA molecules. In the sample chamber, a streptavidin-coated bead was held by an optical trap and the second bead was positioned at the tip of a micropipette through suction (10). The micropipette was fixed to the chamber, which in turn was mounted on a piezoelectric flexure stage (PDQ375; Mad City Lab, Madison, WI), that controlled the position of the pipette with an error <1 nm. A diluted solution of DNA with biotinylated 3′ ends was run through the cell. Once one end of a DNA molecule was attached to the trapped bead, the bead on the pipette was moved toward the trapped bead until the opposite end of the molecule was bound. The procedure is identical to that described by Bennink et al. (31). The extension of the molecule is measured by the movements of the two beads (30). The force is measured by the position of the trapped bead, calibrated by means of viscous drag. A change in force produces a movement of the bead that is measured by the change in the light momentum with a precision of ~0.2 pN (30). The absolute extension of the molecule is estimated at the end of the experiment by moving the pipette toward the trapped bead and measuring the position of the pipette, with 5-nm precision, when the two beads start to separate as judged by the force signal.

Force-clamp experiment

Our system operates either in length- or in force-clamp mode. For length-clamp mode, the feedback signal for the servo system that controls the position of the piezoelectric stage via a proportional, integrative, and differential amplifier is the position sensor of the piezo itself. In the force-clamp mode, the feedback signal for the servo system is the recorded force and the piezoelectric stage moves to compensate for any difference with the desired force. When force is clamped at a constant value, its standard deviation is ≤ 0.3 pN. Force and extension of the molecule are acquired at a rate of 1 kHz. For the experiment, the DNA molecule is first stretched in length-clamp mode at a constant pulling rate of 1.4 μm s^{-1} from the starting unstressed length, until a preset force F_{max}, above the overstretching force, is reached (x_1 in Fig. 1 *a*, attained in 20 s). The system is then switched from length-clamp mode to force-clamp mode and a staircase of force steps (size, ΔF, 0.5–2 pN, interval 5 s) is imposed on the molecule, first in release (negative staircase) down to a force F_{min} below the force for the overstretching transition (x_2 in Fig. 1 *a*, attained in 155 s) and then in stretch (positive staircase, with the same step size and frequency as the negative staircase) up to the preset force F_{max}. At this point (x_3 in Fig. 1 *a*), the system is switched back to the length-clamp mode and the molecule is released at a constant rate to the initial length.

The setting of the proportional, integrative, and differential amplifier controlling the feedback gain is adjusted to minimize the error between the stepwise command signal and the actual force step imposed on the molecule. During the overstretching transition, the complex compliance of the molecule (the sum of the changes in length during and after the force step) becomes quite large and the gain of the proportional amplifier, set for the stiff region of the molecular response, becomes insufficient to preserve a stepwise change in force. On the other hand, presetting from the beginning the feedback gain to the value necessary for the compliant region of the molecular response would cause the gain to be too high for the initial stiff region, which would lead the system to oscillate.

The best possible shape of each step of the positive staircase is attained by evaluating the amplitude of the length response and the deterioration of the force step for each force level during the preceding negative staircase and adjusting consequently the proportional gain of the corresponding step in the subsequent positive staircase. For this reason, the kinetic analysis is based only on the length responses to step increases in force. The performance of the system provides that 1), in the region of the response below and above the overstretching transition, the risetime of the force step is ~2 ms; and 2), in the region of the overstretching transition, the step risetime increases, but even for the responses with the maximum complex

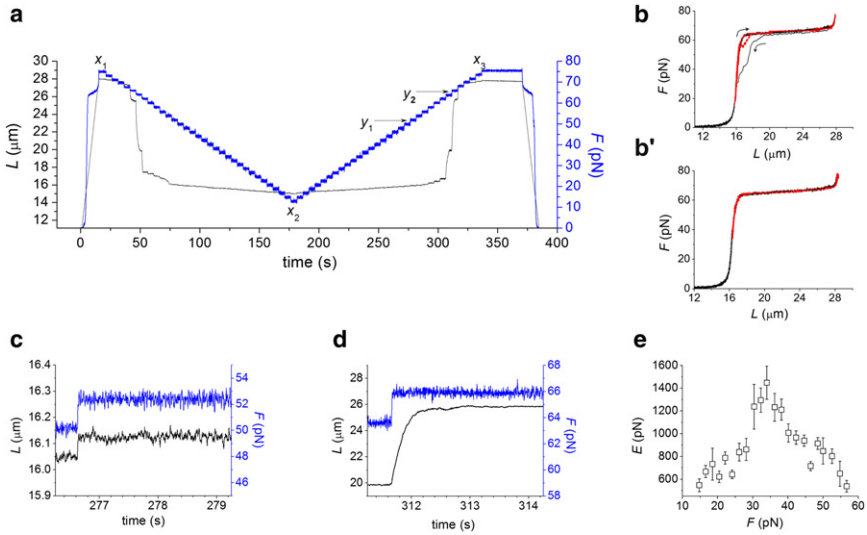

FIGURE 1 Response to stretch-release of ds-DNA in length-clamp mode (ramp-shaped length change) and in force-clamp mode (staircase of 2 pN force steps at 5 s interval). (*a*) Change in length (*black line*) and force (*blue line*) during the protocol used for the experiment. At zero time the molecule is stretched with a ramp in length-clamp mode (velocity 1.4 μm s^{-1}) up to a force of 76 pN (x_1, attained in 20 s) beyond the region of the overstretching transition, that is made evident by the transient reduction in slope of the force-time trace; at x_1 the feedback is switched to force and the molecule is released with the negative staircase of force steps separated by 5-s intervals down to 14 pN (x_2, attained in 155 s) and then stretched with the positive staircase of force steps of similar size and frequency, to attain again 76 pN (x_3); then the feedback is switched back to length and the molecule is released with a ramp-down to zero force (attained in 20 s). (*b* and *b*′) Force-extension curves in length-clamp mode (*black*) and in force-clamp mode (*red*) drawn from a protocol like that in Fig. 1 *a* for either a molecule that shows hysteresis in relaxation (*b*) or a molecule without hysteresis (*b*′). In panel *b* the direction of the length change along the traces is indicated (*closest arrow*). (*c*) Expanded record of the length response (*black*) to the force step (*blue*) 50–52 pN (corresponding to y_1 in Fig. 1 *a*). The length response is purely elastic. (*d*) Expanded record of the length response (*black*) to the force step (*blue*) 64–66 pN (corresponding to y_2 in Fig. 1 *a*). The elastic length change is followed by a slower and much larger elongation with an exponential time course. (*e*) Relation between the elastic modulus (*E*) and force, measured using force steps in the range (15–60 pN) where the molecule in the B-state exhibits an intrinsic elasticity. Data are mean ± SD from 14 molecules with 2 pN step.

compliance, it remains ≤20 ms—that is, one order-of-magnitude shorter than the time constant of the corresponding length response.

An experiment is excluded from the analysis if even only one element of the force staircase deteriorates, so that the stepwise shape is lost.

The size of the force step ΔF was limited to the range 0.5–2 pN, because for $\Delta F < 0.5$ pN the signal/noise ratio was too low, and for $\Delta F > 2$ pN, the number of intermediate transitions was too small. The analysis refers only to data from the 2-pN step (17 molecules) and 0.5-pN step (4 molecules) to maximize the possible effects of the size of the step and thus of the extent of the elongation response on the kinetics of the overstretching transition.

RESULTS AND DISCUSSION

Stretching the DNA molecule by a staircase of force steps

In Fig. 1 *a* the molecule, tethered between two streptavidin-coated beads by means of its biotinylated 3′ ends, is first prestretched in length-clamp mode at constant pulling rate to a length ($L = 28$ μm, x_1 in Fig. 1 *a*) at which the force ($F = 76$ pN) is above the overstretching transition, then the control is switched to force-clamp mode and the molecule is released with a staircase of force steps of 2 pN and 5 s interval down to 14 pN (x_2). The molecule is then stretched with the same force step staircase up to 76 pN (x_3), where the control is switched back to the length-clamp mode and the molecule is released at a constant rate to its unstressed length. During the negative staircase ($x_1 \rightarrow x_2$), the molecule starts to respond according to its intrinsic elasticity in state S and then crosses the region of the overstretching transition that includes five to eight force steps. Conversely, during the positive staircase ($x_2 \rightarrow x_3$), the molecule starts in state B and, once the threshold for the overstretching transition has been attained, takes five to eight force steps to acquire the 100% S state.

The length response to the force step (risetime t_r ~2 ms) in the region of the intrinsic elasticity in state B (y_1 in Fig. 1 *a*, $F = 50$ pN) is shown on expanded vertical and horizontal scales in Fig. 1 *c*. The 2-pN force step induces a stepwise increase in length of ~60 nm, corresponding to a compliance of ~30 nm pN^{-1}. The length response to the same force step in the region of the overstretching transition (y_2 in Fig. 1 *a*, $F = 66$ pN) is shown in Fig. 1 *d* at 10-times lower vertical resolution than in Fig. 1 *c*. In this case, the initial elastic response is followed by a roughly exponential isotonic lengthening of amplitude ~5 μm, complete within the first 500 ms of the 5-s interval.

The force-extension relation obtained from this experiment (Fig. 1 *b*) shows that, at the resolution necessary to describe the whole process, the differences between the two protocols, constant pulling rate (*black line*) and force step staircase (*red line*), emerge only during the relaxation phase; when relaxation is induced by a negative staircase of force steps, the hysteresis in the structural transition is reduced. As suggested by the work of Clausen-Schaumann et al. (15) and Mao et al. (20), this is probably due to the different loading rate preceding the relaxation in either force-clamp or length-clamp. The relaxation obtained with the negative staircase is preceded by a ramp-shaped lengthening that takes a shorter time (20 s) to stretch the molecule, compared to that (155 s) taken by the positive staircase that precedes the length-clamped release, and this minimizes the probability of strand separation.

In 9 of the 17 molecules used for the 2-pN force step, there was no sign of hysteresis during the release with the negative staircase following the length-clamp stretch, and in four of these nine molecules (Fig. 1 *b′*) there was no sign of hysteresis during both releases in force-clamp (*red trace*) and in length-clamp (*black trace*). The chosen mechanical protocol, pulling from different strands, in principle allows strand separation; thus, the lack of such rupture events for molecules overstretched up to 76 pN shows that the DNA can remain double-stranded as it unwinds to achieve the extended conformation. Therefore, melting and generation of conformations more stable than the S-state, such as single-stranded (ss) DNA (15–19), is not a necessary component of the mechanism underlying the overstretching transition.

In the region of forces <60 pN, where the B state of ds-DNA exhibits an intrinsic elasticity, the elastic modulus E can be calculated from the records such as that in Fig. 1 *c*. Elastic modulus E shows a biphasic dependence on the force at which the step is applied (Fig. 1 *e*). In the range of forces 15–35 pN, E increases from 550 ± 50 pN (mean ± SD, 14 molecules with 2 pN steps) to a maximum of 1450 ± 130 pN (10,22,32) and then, in the range of forces 35–57 pN, it reduces again to 530 ± 60 pN. This switching between two kinds of elasticity fits well with the finding that, at forces <35 pN, the twist-stretch coupling of the B state of DNA is negative (that is, the molecule overwinds on stretch), and it becomes positive (that is, the molecule underwinds on stretch) only at higher forces (32).

Load dependence of the extent and rate of the ds-DNA elongation

Above 60 pN, 5–8 steps of 2 pN are necessary to complete the B-S transition (Fig. 1 *a*). The number of steps increases when the step size is reduced, so that there is an inverse proportionality between number and size of the force steps necessary to complete the transition. The elongations elicited by a series of six 2-pN steps, identified by the different colors and the force attained at the end of each step, are shown in Fig. 2 *a*. Going from the first (62 pN, *purple*) to the sixth (72 pN, *green*) step, the amplitude of the elongation (ΔL_e) increases abruptly up to a maximum of ~3.3 μm (third step, 66 pN, *black*) and then reduces again. The initial speed of the elongation does not vary in proportion to its amplitude, so that the duration of the elongation is shorter for the first and sixth step and increases with the amplitude of the elongation. After the elastic response has been subtracted, the time course of the elongation (ΔL) in response to a step increase in force (Fig. 2 *a*) can be interpolated with the exponential equation $\Delta L = \Delta L_e \cdot (1-\exp(-rt))$, where t is the time elapsed after the step, r is the rate constant, and ΔL_e is the asymptotic value of the elongation. The value r is larger at the beginning and at the end of the B-S transition. The dependence of r on the force attained after the 2-pN step is shown for 17 molecules in Fig. 2 *b* (*blue symbols*).

It can be seen that the r points from the four molecules without hysteresis on release (*squares*) superimpose on those from the 13 molecules with hysteresis (*triangles*).

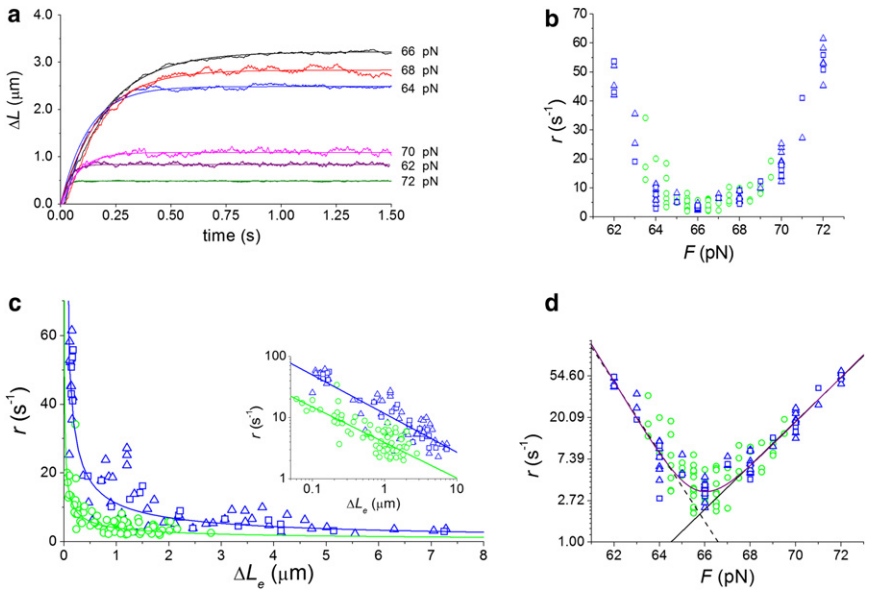

FIGURE 2 Dependence of the extent and rate of elongation on force. (*a*) Superimposed time courses of elongation (ΔL) following the series of 2 pN force steps starting at 60 pN during the staircase. The level of force attained by the step is reported next to the trace. The lines are the exponential fits to the traces as identified by the force level. The rate constants are 47 s^{-1} (62 pN, *purple*), 6.1 s^{-1} (64 pN, *blue*), 3.8 s^{-1} (66 pN, *black*), 5.1 s^{-1} (68 pN, *red*), 9.2 s^{-1} (70 pN, *pink*), and 58 s^{-1} (72 pN, *green*). (*b*) Relationship between the rate of elongation (r) and force (F) following 0.5 pN (*green circles*) and 2 pN (*blue symbols*) force steps. 2 pN data are from 13 molecules showing hysteresis in relaxation (*triangles*) and four molecules without hysteresis (*squares*). (*c*) Relationship between r and the final length change induced by a step ΔL_e for the same data (and *symbols*) as in panel *b*. The lines are the fit on either 2 pN data (*blue*) or 0.5 pN data (*green*) with the power equation $r = C \times \Delta L_e^{b}$. (*Inset*) Same data plotted on a double-logarithmic scale. (*Lines*) Linear regression fit to data: the regression coefficient b is −0.61 ± 0.04 (*blue line*, 2 pN) and −0.55 ± 0.05 (*green line*, 0.5 pN). The parameter b corresponds to the exponent of the power equation in the plot with linear scale. (*d*) Relation between ln r and force for the same data as in panel *b*. (*Black straight lines*) Fits of Eq. 3 (expressing k_+, *continuous line*) to pooled 2 pN and 0.5 pN data in the force range 67–72 pN and Eq. 4 (expressing k_-, *dashed line*) to data in the range 61–65 pN. (*Purple line*) The four-parameter fit (see Eq. S8 and Section S3 in the Supporting Material) to pooled 2 pN and 0.5 pN data.

The *r-F* relation is U-shaped, showing maxima of ~50 s^{-1} at the beginning ($F \sim 62$ pN) and at the end ($F \sim 72$ pN) of the overstretching transition and a minimum of 3.82 ± 0.68 s^{-1} (mean ± SD, calculated in the range 65.5–66.5 pN) in the plateau region. The relation obtained from four molecules for which the size of the step in the staircase was 0.5 pN (*green circles*) almost superimposes on that with 2 pN steps (*r* in the range 65.5–66.5 pN is 3.94 ± 1.52 s^{-1}, the same as that obtained with the 2 pN step), indicating that *r* is independent of the force step size and depends only on the final force attained during the step. The monotonic increase of the total length of the molecule *L* with the increase in force (Fig. 1 *b*) also implies that the *r-L* relation is U shaped (see Fig. S2 in the Supporting Material).

The findings that the rate of elongation has the same U-shaped relation when plotted against either the force (Fig. 2 *b*) or the length of the molecule (see Fig. S2), independently of the size of the force step, are direct indications that the response is an intrinsic property of the molecule, related to its transition kinetics. Further discussion of the possible contributions of either the translational drag of the bead or the rotational drag of the molecule while untwisting, is reported in detail in section S1 in the Supporting Material.

The amplitude of the elongation (ΔL_e) following the force step varies with force in a way that is a mirror image of the rate. The maximum elongation occurs in the central region of the overstretching transition: in the range 65.5–66.5 pN, where *r* is minimum, ΔL_e is 5.03 ± 1.63 μm for the 2-pN step and 1.34 ± 0.51 μm for the 0.5-pN step. The relationship between *r* and ΔL_e appears hyperbolic (Fig. 2 *c*) with a larger curvature for the smaller force step. A log-log plot of this relation shows that, whatever the size of the force step, *r* is related to ΔL_e through the power equation: $r = C \cdot \Delta L_e{}^b$, where *b* is ~−0.6 (the regression coefficient *b* is -0.61 ± 0.04 and -0.55 ± 0.05 for the 2-pN and 0.5-pN steps, respectively). In this case it can be demonstrated that the elongation following a force step in the region of the overstretching transition is consistent with a two-state reaction with first-order kinetics (see section S2 in the Supporting Material). Moreover, the downward shift observed for the smaller force step (corresponding to a reduction of *r* by 3.5 times for $\Delta L_e = 1$ μm) indicates once again that the rate of elongation is not determined by the extent of elongation—a result that confirms that the rotational drag of the molecule while untwisting is not the parameter that determines the kinetics of the process (see section S1B in the Supporting Material).

The transition pathway

DNA overstretching at 25°C may show hysteresis (Fig. 1 *b*), which is interpreted as an indicator of melting and strand separation (unpeeling). Unpeeling has also been proposed as a fundamental component of overstretching. For example, in Whitelam et al. (21) the presence of asymmetry in the hysteresis of the force-extension curve as well as the high rigidity (22,25) and helicity (9,10,12,14) of the extended DNA state was reproduced using a four-state model that includes a basepaired B state, a basepaired S state, a molten state, and a unpeeled state. With our stretch-release protocol, a limited hysteresis is seen upon release in most cases (Fig. 1 *b*), which indicates that a certain amount of unpeeling takes place during the overstretching phase. Twenty-percent of the investigated molecules, however, do not show any hysteretic behavior (Fig. 1 *b′*), which is an indication that, under our experimental conditions, unpeeling is not a necessary condition for overstretching to occur and generate an extended S state of ds-DNA.

Moreover, the transition kinetics are not affected by the presence or absence of hysteresis (compare *blue triangles* and *squares* in Fig. 2, *b–d*). We therefore conclude that the transition rates measured here depict the transition between the B and S forms of ds-DNA, without any effect of other competing structural transitions, such as unpeeling. These other transitions therefore do not represent rate-limiting steps for the overstretching process. Thus, consistent with the observations of Fu et al. (25), also under our free end conditions, if strand separation occurs, it occurs after the complete transition to the S form has occurred.

Finally, note that the probability for the strand separation and the hysteretic behavior following DNA overstretching is likely to increase with the presence of nicks, which in turn would reduce the length of the DNA segments rotating as a whole, following a force step. Under these conditions the finding that the transition kinetics in the overstretching region are not related to the subsequent hysteretic behavior, and thus to the length of the rotating segments, further supports the conclusion that the elongation kinetics are not affected by the rotational drag (see section S1B in the Supporting Material).

The structure of the transition state

According to a two-state model, ds-DNA is composed of an ensemble of units which can attain two different conformational states—a compact B state characterized by a molecular extension of 0.33 nm per bp, and an extended S state characterized by a molecular extension of 0.56 nm per bp. The molecular extension of each of these units provides a convenient reaction-coordinate to study the overstretching transition. The free energy profile of each unit along this reaction coordinate, schematically represented in Fig. 3, is dictated by four fundamental parameters: the free energy difference between compact and extended state ΔG, the forward energy barrier $\Delta G^{\ddagger}{}_{+}$, the backward barrier being $\Delta G^{\ddagger}{}_{-} = \Delta G^{\ddagger}{}_{+} - \Delta G$, and the distance of the transition state from both the compact state $x^{\ddagger}{}_{+}$ and the extended state $x^{\ddagger}{}_{-}$.

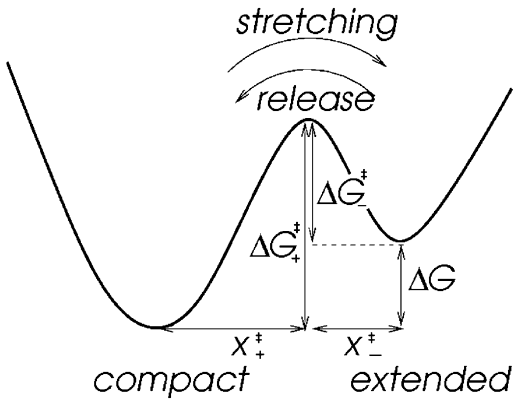

FIGURE 3 Pictorial representation of the free energy landscape of a two-state unit. ΔG, free energy difference between the compact state and the extended state; $\Delta G^{\ddagger}_{+}$, energy barrier for the forward transition; $\Delta G^{\ddagger}_{-}$, energy barrier for the backward transition. The distance of the transition state from the compact state is $x^{\ddagger}_{+}$ and from the extended state is $x^{\ddagger}_{-}$.

In this case, the rate constants for the elongation (k_+) and the shortening (k_-) of the molecule depend exponentially on the force according to Kramers-Bell theory:

$$k_+ = A_+ \cdot \exp\left(\frac{F \cdot x^{\ddagger}_{+}}{k_B T}\right), \quad (1)$$

$$k_- = A_- \cdot \exp\left(-\frac{F \cdot x^{\ddagger}_{-}}{k_B T}\right), \quad (2)$$

where $x^{\ddagger}_{+}$ and $x^{\ddagger}_{-}$ (nm) are the distances to the transition state from the compact and the extended states, respectively; k_B is the Boltzmann constant; T is the temperature in Kelvin; and A_+ and A_- (s^{-1}) are the rate constants at zero force (see section S2 in the Supporting Material).

The unidirectional rate constants expressed in logarithmic units have a linear dependence on force and the slope of the relation is the distance from the starting state to the transition state divided by $k_B T$:

$$\ln k_+ = \ln A_+ + \left(\frac{F \cdot x^{\ddagger}_{+}}{k_B T}\right), \quad (3)$$

$$\ln k_- = \ln A_- - \left(\frac{F \cdot x^{\ddagger}_{-}}{k_B T}\right). \quad (4)$$

In our experiments, the observed rate constant r (Fig. 2 *b*) is the sum of the forward and reverse rate constants. However, because the equilibrium is dominated by k_- in the low force side of the overstretching transition and by k_+ in the high force side, we used the logarithmic relations in these two regions to separately estimate the slopes of the respective unidirectional reactions and thus of the distances to the transition state (Fig. 2 *d*). The parameters of the linear regression equations fitted to ln r with Eq. 3 in the force range 67–72 pN and Eq. 4 in the range 61–65 pN are reported in Table 1 either for the 0.5-pN steps (*green circles*) or for the 2-pN steps (*blue symbols*). In either case all the kinetic parameters are not significantly influenced by the force step size ($P > 0.1$). The linear fits on the pooled 0.5 pN and 2 pN data within the same force ranges give similar values: ln $A_+ = -34.14 \pm 1.11$ and $x^{\ddagger}_{+} = 2.18 \pm 0.07$ nm for Eq. 3 (*black continuous line*); ln $A_- = 56.05 \pm 2.99$, $x^{\ddagger}_{-} = 3.67 \pm 0.19$ nm for Eq. 4 (*black dashed line*).

Alternatively, a more complex, four-parameter fit with the expression of the relaxation rate $r = k_+ + k_-$ (see Eq. S8 and section S3 in the Supporting Material) can be performed on the entire force range (*purple line* in Fig. 2 *d*) and gives values of the four parameters A_+, A_-, $x^{\ddagger}_{+}$, and $x^{\ddagger}_{-}$ that are almost identical to those determined here by fitting separately the low and high force branches of the relation.

From the estimated distances to the transition state, $x^{\ddagger}_{+}$ and $x^{\ddagger}_{-}$, we conclude that the transition occurs roughly midway between the B state and the S state of DNA, slightly shifted toward the B state. The sum of the two distances, $(x^{\ddagger}_{+} + x^{\ddagger}_{-})$, gives a total length change for the elementary reaction Δx of 5.85 ± 0.20 nm. The ratio of Δx over the elongation undergone by each bp ($0.33 \times 1.7 - 0.33 = 0.231$ nm) measures the number of bp involved in the elementary reaction, or cooperativity coefficient, and is 25.32 ± 0.86.

Thus, the B-S transition can be explained by the two-state reaction model, where different regions of DNA independently undergo the transition. However, an alternative nucleation-diffusion mechanism might be considered in which, following a nucleation event consisting of a B-S transition in a local region, the S-portion of the molecule extends by propagating its boundaries at the expenses of the B-portion. These two mechanisms could also act in combination in a hybrid mechanism, in which nucleation events take place independently in different regions. The exponential time course of the elongation following a force step (Figs. 1 *d* and 2 *a*) strongly suggests that the two-state reaction mechanism is dominant, because a purely nucleation–propagation mechanism would be characterized by a linear time course. Further support for the two-state model is given in section S2 in the Supporting Material, where we show that it accurately reproduces the observed relationship between elongation rate and amplitude (Fig. 2 *c*).

TABLE 1 Kinetic parameters of the two-state reaction estimated with Eqs. 3 and 4

Force step (pN)	Eq. 3		Eq. 4	
	ln A_+	$x^{\ddagger}_{+}$ (nm)	ln A_-	$x^{\ddagger}_{-}$ (nm)
0.5	-32.39 ± 6.59	2.07 ± 0.39	64.11 ± 12.01	3.91 ± 0.77
2	-34.45 ± 1.27	2.18 ± 0.07	60.75 ± 3.46	3.72 ± 0.23
Pooled	-34.1 ± 1.11	2.18 ± 0.07	56.05 ± 2.99	3.67 ± 0.19

The extent of variability of the size of the cooperatively overstretching units that is compatible with the observed equilibrium kinetics (the force-extension relation) and relaxation kinetics (the force dependence of the rate of elongation following a force step) is examined in section S4 in the Supporting Material. We demonstrate that a stochastic variability up to 30% in either x_+ or x_- does not substantially affect either kinetic parameter. Instead, the variability of either the free-energy barrier $\Delta G^{\ddagger}_{+}$ or the free energy change ΔG must be lower than 10%.

The finding that the transition state is almost midway between the compact and extended states implies that the force (F_m) at which the relaxation rate is minimum also corresponds, within our resolution limit, to the force (F_e) at which the work done for the elongation (W_e) equals the free energy difference between the compact and the extended states: $W_e = F_e \cdot \Delta x$ (see section S2 in the Supporting Material). With $\Delta x = 5.85$ nm, W_e per elementary elongation step is ($66 \times 5.85 =$) 386 zJ per molecule (or 236 kJ per mol), that at 25°C corresponds to 94 k_BT. The average binding free energy per bp obtained from these mechanical measurements is ($F_e \cdot 0.231$ nm $=$) 15.25 zJ, corresponding to only 3.71 k_BT per molecule. The cooperative mechanism for DNA elongation increases the stability of the DNA structure in the B state by increasing the minimal free energy change necessary for the elongation reaction to 94 k_BT.

Comparison with recent experiments

The exponential kinetics observed for λ-DNA apparently contrasts with the results of other recent overstretching experiments under force-clamp. Fu et al. (25) report on constant force DNA overstretching experiments performed by means of magnetic tweezers. Under melting-preventing conditions (high salt concentration or moderately GC-rich sequences), DNA constructs of ~600 bp show, in response to force increase, lengthening followed by length fluctuations, instead of a smooth exponential elongation. To assess the predictions of our two-state model for such conditions, we performed a series of Monte Carlo simulations. A set of 23 two state units, each 25-bp-long, was defined to simulate a molecule 575-bp-long. All units were initially assigned a compact conformation and force was gradually increased with 1-pN steps.

For each force value, the system was integrated for 20 s according to a stochastic dynamics where each unit could change its state from compact to extended and from extended to compact according to their transition probabilities computed as $k_{\pm}\ dt$ with dt the integration time. The values $k_{\pm}$ were computed according to Eqs. 1 and 2 using the parameters resulting from the fit of the rate-force relation as in Fig. 2, *a* and *b*. Fig. 4 *a* confirms that, for a molecular size as low as 575 bp, random length fluctuations are so prevalent to mask almost completely the shape of the relaxation. On the contrary, as shown in Fig. 4 *b*, that reports the result of a simulation with 1936 two-state units, or ($1936 \times 25 =$) 48,400 bp, the entire DNA molecule exhibits a much smoother lengthening, that with an adequately expanded timescale (see *inset* in Fig. 4 *b*), reveals its exponential kinetics. This is due to the self-averaging effect of length fluctuations in the units in a linear chain when the number of units is sufficiently high: for each extending unit, another one contracts, compensating the effect of the first. A striking result of this simulation is that the number of bp involved in the elementary reaction, selected for fitting the responses of a molecule 48-kbp long with the two-state model, is able to predict to a very good approximation the length fluctuations measured by Fu et al. (25) for molecules two orders-of-magnitude shorter.

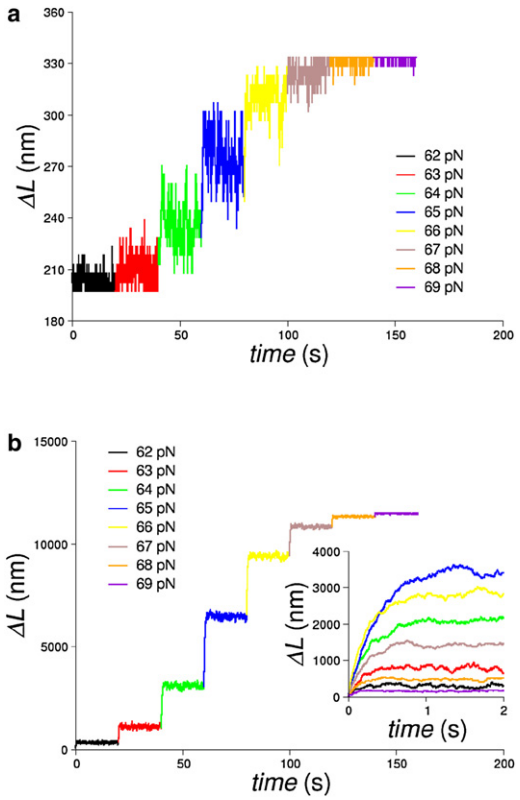

FIGURE 4 Simulated time course of eight consecutive length changes in response to staircased 1-pN force steps. The responses are calculated for a system composed of identical two-state units of 25 bp. (*a*) Twenty-three two-state units (575 bp, as in Fu et al. (25)); (*b*) 1936 two-state units (48,400 bp). Different colors correspond to different force values from 62 to 69 pN. (*Inset*) Superposed length responses on a faster time base, adequate to resolve the exponential time course. This indicates that the stepwise length changes in Fu et al. (25) are due to the absence of time resolution in those experiments.

CONCLUSION

The extended state of ds-DNA

The results of this work give a solid basis to the definition of the S state of ds-DNA, showing that 100% of the extended

form of DNA generated during the overstretching transition remains double-stranded and is produced in a perfectly reversible way via intermediate state transitions. This conclusion agrees with the recent evidence that topologically closed ds-DNA can also undergo the overstretching transition at ~65 pN (23). In a molecule free to rotate or unpeel, further transitions to the more stable ss-DNA are not directly responsible for the overstretching transition and would take place either on a longer timescale or under the action of melting promoting factors such as temperature, pH, and ionic strength (15–17,21,22,25,33). Thus, the strand separation during the overstretching transition recently demonstrated with fluorescence microscopy (18,19), was likely to have been promoted at some stage of the molecule manipulation used in those experiments.

The first description in this work of the elongation kinetics of intermediate states within the overstretching region (Fig. 2) together with the demonstration that the force-extension relation at equilibrium may be perfectly reversible (Fig. 1 b') indicate, in agreement with previous work, that the whole interconversion from the B to the S state occurs while preserving the double-stranded structure. Moreover, recording the exponential kinetics of elongation and their load dependence allows the two-state nature of the B-S transition mechanism to be defined. Under these conditions we explain both transient and equilibrium responses in terms of a two-state reaction that allows the size of the elementary reaction (Δx ~5.8 nm) and thus the degree of bp cooperativity (~25 bp) to be defined, and provides some structural insight into the transition state.

The definition of the kinetics and energetics of the B-S transition of ds-DNA in this work represents a significant contribution to understanding the biological role of the S state in the interplay between mechanics and enzymology of DNA-protein complexes. DNA overstretching promotes the nucleation/polymerization on the DNA of the RecA protein (34), which is a prerequisite for homologous recombination between two DNA segments (35). However, the extended form of ds-DNA is also likely to be involved in the regulation of other basic functions of the DNA-protein machinery.

X-ray crystallography (36) has allowed the structural details of the boundary between the B state and the Z state, the left-handed conformation associated with the transcription start site, to be described (37,38). The crystallographic approach is possible because the B-Z transition occurs under no- or low-load conditions and for slightly negative torque values that are likely induced (or stabilized) by the Z-DNA binding proteins (39). Instead, according to the force-torque phase diagram in Sarkar et al. (13), the boundary for the S-Z transition lies in a region of higher loads and more negative torques.

This implies that, even with the molecule under stress, the torque contribution by the DNA-binding protein may not be adequate for promoting the transition or, in other words, that in the S state the formation of the transcription start site is inhibited, because in this state the DNA is more resistant than in the B state to the effect of the negative torque. At the same time, the position of the boundary for the S-Z transition in the phase diagram of Sarkar et al. (13) makes it explicit that the S-Z transition can only be studied by integrating time-resolved structural and mechanical methods and not by x-ray crystallography, because the stress on the DNA molecule cannot be reproduced in crystals. In this respect, the present description of the load dependence of kinetics and energetic of the B-S transition is an important step forward in understanding the role of the S state in gene regulation and expression.

SUPPORTING MATERIAL

Additional sections with five figures are available at http://www.biophysj.org/biophysj/supplemental/S0006-3495(11)00769-7.

We thanks Malcolm Irving and Gabriella Piazzesi for comments on the manuscript.

This work was supported by Ente Cassa di Risparmio di Firenze (Italy) and by Italian Institute of Technology (SEED-MYOMAC 2009).

REFERENCES

1. Bustamante, C., Z. Bryant, and S. B. Smith. 2003. Ten years of tension: single-molecule DNA mechanics. *Nature.* 421:423–427.
2. Allemand, J. F., D. Bensimon, and V. Croquette. 2003. Stretching DNA and RNA to probe their interactions with proteins. *Curr. Opin. Struct. Biol.* 13:266–274.
3. Smith, S. B., L. Finzi, and C. Bustamante. 1992. Direct mechanical measurements of the elasticity of single DNA molecules by using magnetic beads. *Science.* 258:1122–1126.
4. Bustamante, C., J. F. Marko, …, S. Smith. 1994. Entropic elasticity of λ-phage DNA. *Science.* 265:1599–1600.
5. Marko, J. F., and E. D. Siggia. 1995. Stretching DNA. *Macromolecules.* 28:8759–8770.
6. Baumann, C. G., S. B. Smith, …, C. Bustamante. 1997. Ionic effects on the elasticity of single DNA molecules. *Proc. Natl. Acad. Sci. USA.* 94:6185–6190.
7. Strick, T. R., J. F. Allemand, …, V. Croquette. 1998. Behavior of supercoiled DNA. *Biophys. J.* 74:2016–2028.
8. Bouchiat, C., M. D. Wang, …, V. Croquette. 1999. Estimating the persistence length of a worm-like chain molecule from force-extension measurements. *Biophys. J.* 76:409–413.
9. Cluzel, P., A. Lebrun, …, F. Caron. 1996. DNA: an extensible molecule. *Science.* 271:792–794.
10. Smith, S. B., Y. Cui, and C. Bustamante. 1996. Overstretching B-DNA: the elastic response of individual double-stranded and single-stranded DNA molecules. *Science.* 271:795–799.
11. Strick, T. R., J. F. Allemand, …, V. Croquette. 1996. The elasticity of a single supercoiled DNA molecule. *Science.* 271:1835–1837.
12. Léger, J. F., G. Romano, …, J. F. Marko. 1999. Structural transitions of a twisted and stretched DNA molecule. *Phys. Rev. Lett.* 83:1066.
13. Sarkar, A., J. F. Léger, …, J. F. Marko. 2001. Structural transitions in DNA driven by external force and torque. *Phys. Rev. E.* 63:051903.
14. Bryant, Z., M. D. Stone, …, C. Bustamante. 2003. Structural transitions and elasticity from torque measurements on DNA. *Nature.* 424: 338–341.

15. Clausen-Schaumann, H., M. Rief, …, H. E. Gaub. 2000. Mechanical stability of single DNA molecules. *Biophys. J.* 78:1997–2007.

16. Williams, M. C., J. R. Wenner, …, V. A. Bloomfield. 2001. Entropy and heat capacity of DNA melting from temperature dependence of single molecule stretching. *Biophys. J.* 80:1932–1939.

17. Wenner, J. R., M. C. Williams, …, V. A. Bloomfield. 2002. Salt dependence of the elasticity and overstretching transition of single DNA molecules. *Biophys. J.* 82:3160–3169.

18. van Mameren, J., P. Gross, …, E. J. Peterman. 2009. Unraveling the structure of DNA during overstretching by using multicolor, single-molecule fluorescence imaging. *Proc. Natl. Acad. Sci. USA.* 106:18231–18236.

19. Williams, M. C., I. Rouzina, and M. J. McCauley. 2009. Peeling back the mystery of DNA overstretching. *Proc. Natl. Acad. Sci. USA.* 106:18047–18048.

20. Mao, H., J. R. Arias-Gonzalez, …, C. Bustamante. 2005. Temperature control methods in a laser tweezers system. *Biophys. J.* 89:1308–1316.

21. Whitelam, S., S. Pronk, and P. L. Geissler. 2008. There and (slowly) back again: entropy-driven hysteresis in a model of DNA overstretching. *Biophys. J.* 94:2452–2469.

22. Cocco, S., J. Yan, …, J. F. Marko. 2004. Overstretching and force-driven strand separation of double-helix DNA. *Phys. Rev. E.* 70:011910.

23. Paik, D. H., and T. T. Perkins. 2011. Overstretching DNA at 65 pN does not require peeling from free ends or nicks. *J. Am. Chem. Soc.* 133:3219–3221.

24. Fu, H., H. Chen, …, J. Yan. 2010. Two distinct overstretched DNA states. *Nucleic Acids Res.* 38:5594–5600.

25. Fu, H., H. Chen, …, J. Yan. 2010. Transition dynamics and selection of the distinct S-DNA and strand unpeeling modes of double helix overstretching. *Nucl. Acids Res.* 10.1093/nar/gkq1278.

26. Michaelis, J., A. Muschielok, …, J. R. Moffitt. 2009. DNA based molecular motors. *Phys. Life Rev.* 6:250–255.

27. Whitelam, S., S. Pronk, and P. L. Geissler. 2008. Stretching chimeric DNA: a test for the putative S-form. *J. Chem. Phys.* 129:205101.

28. Stigter, D. 1998. An electrostatic model of B-DNA for its stability against unwinding. *Biophys. Chem.* 75:229–233.

29. Cizeau, P., and J.-L. Viovy. 1997. Modeling extreme extension of DNA. *Biopolymers.* 42:383–385.

30. Smith, S. B., Y. Cui, and C. Bustamante. 2003. Optical-trap force transducer that operates by direct measurement of light momentum. *Methods Enzymol.* 361:134–162.

31. Bennink, M. L., O. D. Schärer, …, J. Greve. 1999. Single-molecule manipulation of double-stranded DNA using optical tweezers: interaction studies of DNA with RecA and YOYO-1. *Cytometry.* 36:200–208.

32. Gore, J., Z. Bryant, …, C. Bustamante. 2006. DNA overwinds when stretched. *Nature.* 442:836–839.

33. Danilowicz, C., C. Limouse, …, M. Prentiss. 2009. The structure of DNA overstretched from the 5′5′ ends differs from the structure of DNA overstretched from the 3′3′ ends. *Proc. Natl. Acad. Sci. USA.* 106:13196–13201.

34. Hegner, M., S. B. Smith, and C. Bustamante. 1999. Polymerization and mechanical properties of single RecA-DNA filaments. *Proc. Natl. Acad. Sci. USA.* 96:10109–10114.

35. West, S. C. 1992. Enzymes and molecular mechanisms of genetic recombination. *Annu. Rev. Biochem.* 61:603–640.

36. Ha, S. C., K. Lowenhaupt, …, K. K. Kim. 2005. Crystal structure of a junction between B-DNA and Z-DNA reveals two extruded bases. *Nature.* 437:1183–1186.

37. Liu, R., H. Liu, …, K. Zhao. 2001. Regulation of CSF1 promoter by the SWI/SNF-like BAF complex. *Cell.* 106:309–318.

38. Oh, D. B., Y. G. Kim, and A. Rich. 2002. Z-DNA-binding proteins can act as potent effectors of gene expression in vivo. *Proc. Natl. Acad. Sci. USA.* 99:16666–16671.

39. Schwartz, T., M. A. Rould, …, A. Rich. 1999. Crystal structure of the Zα domain of the human editing enzyme ADAR1 bound to left-handed Z-DNA. *Science.* 284:1841–1845.